ECONOMIC SEISMIC LOSS ASSESSMENT OF RC SCHOOL BUILDINGS IN SOUTH KOREA

I.S. Choi[(1)], J.H. Kim[(2)], H.J. Chang[(3)], J.H. Sohn[(4)]

[(1)] *Ph.D Candidate, Department of Architecture and Architectural Engineering, Yonsei University, Seoul 03722, Republic of Korea, insub@yonsei.ac.kr*
[(2)] *Associate Professor, Department of Architecture and Architectural Engineering, Yonsei University, Seoul 03722, Republic of Korea, junhkim@yonsei.ac.kr*
[(3)] *Ph.D Candidate, Department of Architecture and Architectural Engineering, Yonsei University, Seoul 03722, Republic of Korea, insub@yonsei.ac.kr*
[(4)] *M.S Student, Department of Architecture and Architectural Engineering, Yonsei University, Seoul 03722, Republic of Korea, kurtsohn@yonsei.ac.kr*

Abstract

Economic seismic loss assessment for evaluating seismic risk is becoming important in South Korea, since earthquake damages had been occurred in building structures caused by major two earthquakes (2016 Gyeongju earthquake, ML 5.8; 2017 Pohang earthquake, ML 5.4). The main purpose of this study is to develop a methodology to evaluate customized economic seismic loss in South Korea. RC school buildings with masonry infills are selected as the case study model, because the past two earthquakes caused large economic loss in the school buildings than in other buildings. The FE model was presented to simulate the short column effect that causes premature failure of the columns by concentrating on shear stress. The seismic fragility curves for the structural and nonstructural components were derived from nonlinear time history analysis. The repair costs of the structural and nonstructural components were defined to produce a customized economic seismic loss function through statistical data on the construction cost of RC school buildings. Using the seismic fragility curves and the repair costs, this study developed a customized economic seismic loss function. In addition, loss-based seismic performance criteria were established to directly correlate the current code-defined (i.e. displacement-based) seismic performance criteria. Then, the loss-based seismic performance of RC school buildings in Pohang city were estimated. The proposed methodology can provide decision-making data for evaluating seismic performance based on seismic loss and has the potential to extend to loss assessment of other categories of buildings.

Keywords: economic seismic loss; RC school buildings; seismic resilience; loss estimation

1. Introduction

It is practically known from past earthquakes that earthquake disasters cause many economic losses in building structures. Seismic risk assessment of the building structures is essential to secure seismic resilience of global or local communities in the future by predicting the seismic losses induced by the earthquake disasters. The seismic risk assessment of the building structures can be evaluated on the basis of the seismic loss assessment of the building structures, which are expected to be caused by the earthquake disasters.

The performance-based seismic design methods [1, 2], developed and started to be used in the mid-1990s, divides the performance of the building structures into four categories (operational, immediately occupancy, life safety, and collapse prevention) based on structural damages. Although the performance level of the building structures was estimated probabilistic methods by fragility analysis for structural components [3], it is difficult to directly link the damage probability and the seismic losses of the building structures. In fact, according to the Earthquake Damage Survey report [4, 5], it is found that the damage to nonstructural components accounts for more than the direct economic loss of buildings rather than structural damages. Therefore, in order to derive decision-making corresponding to the observed loss, it is necessary to consider the direct economic loss comprised of the structural and nonstructural components [6].

In South Korea, two major earthquakes (5.8M_L Gyeongju earthquake in 2016 and 5.4M_L Pohang earthquake in 2017) have increased interest in ensuring the safety of the building structures against the earthquake disasters. The survey of the building structures damaged by the two earthquakes revealed that school building structures belonging to the essential facility were vulnerable to the earthquakes [7, 8]. The building structures that have suffered significant damages from the two earthquakes have almost no seismic design applied, and generally the building structures with no seismic design are known to be vulnerable to the earthquakes due to premature shear failure of column. In other words, it is important to evaluate seismic losses for school buildings that are not seismically designed for future seismic events.

Seismic vulnerability function (i.e. seismic loss function) can be used as a tool to evaluate the monetary losses resulted from the physical damages. The seismic losses of nonstructural components account for more than 80% of the total seismic losses of building structures in the case of commercial building structures [9]. Therefore, it is necessary to evaluate the seismic fragility of nonstructural components to assess the seismic losses. Analyzing the existing research [10-13] to estimate the seismic fragility for various nonstructural components, most research have been conducted to define the engineering demand parameters (EDPs) and limit states of nonstructural components through static or dynamic experimental test. These existing research provide the analytical methods and experimental data for deriving the seismic fragility functions of the structural and nonstructural components, but there are some limitations to overcome: (i) it is necessary to define the seismic fragility functions that reflect the structural characteristics of school building in South Korea; (ii) integrated seismic fragility functions are required for structural and nonstructural components; (iii) the seismic fragility functions for each components can be defined for each story level, not for the building level, to evaluate precise seismic damage evaluation; (iv) the seismic vulnerability function for individual building is required to estimate the earthquake-induced loss.

Therefore, this study aimed to develop a framework for evaluating the seismic vulnerability function considering the fragility function of structural and nonstructural regarding each story level. The school building structures are selected the case study model. Nonlinear model for the column elements was presented to simulate the flexure-shear behavior of the building structure and was verified through comparison with the existing experimental data. The probabilistic seismic demand models for each story were established by using the maximum interstory drift ratio and the maximum peak floor acceleration through time history analysis. The seismic fragility functions for the case study model were estimated using the seismic demand model for each component. The seismic vulnerability function for the prototype model was defined using the seismic fragility functions obtained by simulation method. Also, loss-based seismic performance criteria were defined by correlation analysis with the current code-defined (i.e. displacement-based) seismic performance criteria to evaluate the loss-based seismic performance of the building structures.

© The 17th World Conference on Earthquake Engineering

2. Prototype Model Description

The seismic losses due to the 2017 Pohang earthquake were analyzed to select the prototype model that is vulnerable to earthquakes. Since public buildings are classified as essential facilities, which should be secured structural safety during disasters such as earthquakes, the seismic losses of public facilities were analyzed as shown in Table 1. According to the analysis of the loss of public facilities in the Pohang earthquake in 2017, school buildings account for about 48.2% of the total public loss. Securing seismic performance is important because school buildings are used as shelters during earthquakes. However, school buildings located the region are vulnerable to earthquake disaster. So, the school building structures were selected as the case study building structures in this study.

Table 1 – Seismic loss data of public facilities induced by Pohang earthquake (source from [14])

Division	Seismic Loss		
	₩	$	%
Infrastructures	4,993,712,000	4,161,427	18.6
School buildings	12,932,970,000	10,770,475	48.2
Hospital buildings	2,133,661,000	1,778,051	7.9
ETC†	6,802,731,000	5,668,943	25.3

† ETC includes military and small facilities.

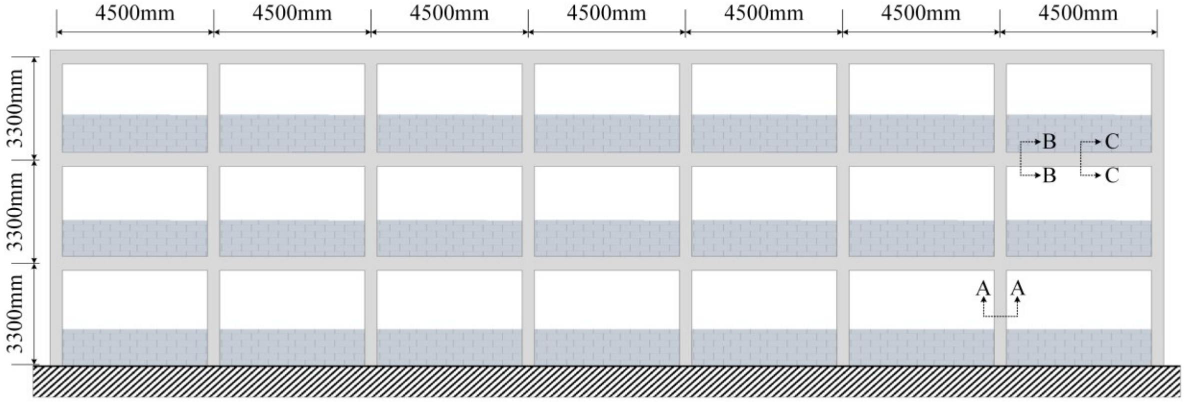

<Elevation of prototype model>

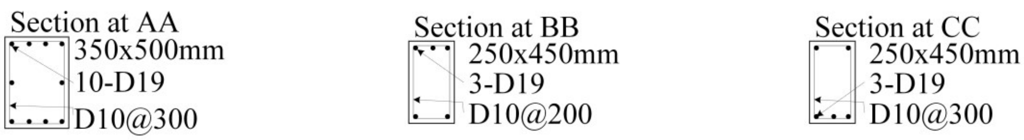

<Section of structural elements>

Fig. 1 – Detail of prototype model of the school building structure

Since the school buildings were classified as essential facility and applied seismic design code after revision of seismic design code in 2005, most school buildings located South Kore do not have sufficient seismic performance. In order to determine the prototype model of the school building, reference (school building standard blueprint [15]) was investigated. A three-story and seven-span RC moment frame with unreinforced masonry infills was selected as the prototype model, as shown in Fig. 1. The properties of the concrete and steel materials were determined considering the construction year (1973-1988) of the real building structures as specified in a guideline for seismic performance evaluation [16]. Concrete compressive strength is f_c' = 15MPa and steel yielding strength is f_y = 240MPa. The dead load is 3.7kN/m^2 and the live load is 3.0kN/m^2.

© The 17th World Conference on Earthquake Engineering

3. Numerical Model of the School Building

3.1. General

The nonlinear modeling for structural elements was performed to simulate the time history analysis of the case study building structure. OpenSees [17], finite element simulation program, was used to perform nonlinear modeling and time history analysis of the prototype model. School buildings are more likely to cause premature shear failure due to the short column effect resulted from the masonry infills between the columns.

The frame elements are modeled to simulate the flexure-shear behavior of the column elements as shown in Fig. 2. One of the typical structural characteristic of school building is that the masonry infills between columns classified as nonstructural components affects the structural behavior. Therefore, even though the masonry infills are classified as nonstructural components, nonlinear analysis is performed by adding modeling of masonry infills to the numerical model. The consideration of numerical model in columns and masonry infills is describe as follow.

Columns. The flexural-shear model composed of fiber element and shear spring was used to simulate the seismic behavior of the column elements considering the premature shear failure. In this model, the flexural behavior of the column is simulated by the fiber element, and the shear behavior of the column is simulated by the shear spring. The details of the column modeling will be discussed in Section 3.2.

Masonry infills. Equivalent diagonal struct element (i.e. lumped plasticity model) with nonlinear axial spring and linear truss elements was used. Existing studies [18, 19] have reported that the equivalent diagonal struct suggested by FEMA 356 [20] simulates the behavior of masonry infills closest to the actual behavior. The modeling parameters for the equivalent diagonal struct are discussed in Section 3.3.

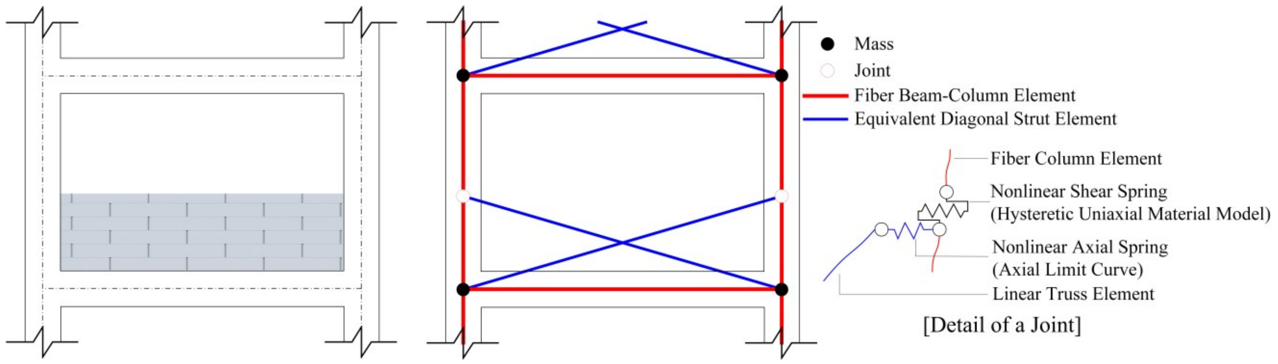

(a) A frame module (b) Detail of the numerical model

Fig. 2 – Total response of column element considering flexure-shear behavior

3.2. Column flexure-shear model

The fiber element that can express the flexural behavior of the column elements is modeled as a five node element by dividing the confined and unconfined regions (see Fig. 3(a)). A linear tension softening model (Concrete02) by Hisham M. was used as the concrete material model, and the Giuffré-Menegotto-Pinto model (Steel02) was used as the steel material model in OpenSees.

The shear spring model to simulate the shear behavior of the column elements is shown in Fig. 3(b). Shear strength, V_y, was estimated using equation (1) presented in FEMA 356 [20], and shear deformation, Δ_y, was calculated by considering the effective stiffness of the column. The detail information can be founded in FEMA 356.

© The 17th World Conference on Earthquake Engineering

$$V_y = k_1 \frac{A_v f_y d}{s} + \lambda k_2 \left(\frac{0.5\sqrt{f_c'}}{M/Vd} \sqrt{1 + \frac{P}{0.5\sqrt{f_c'}A_g}} \right) 0.8A_g \tag{1}$$

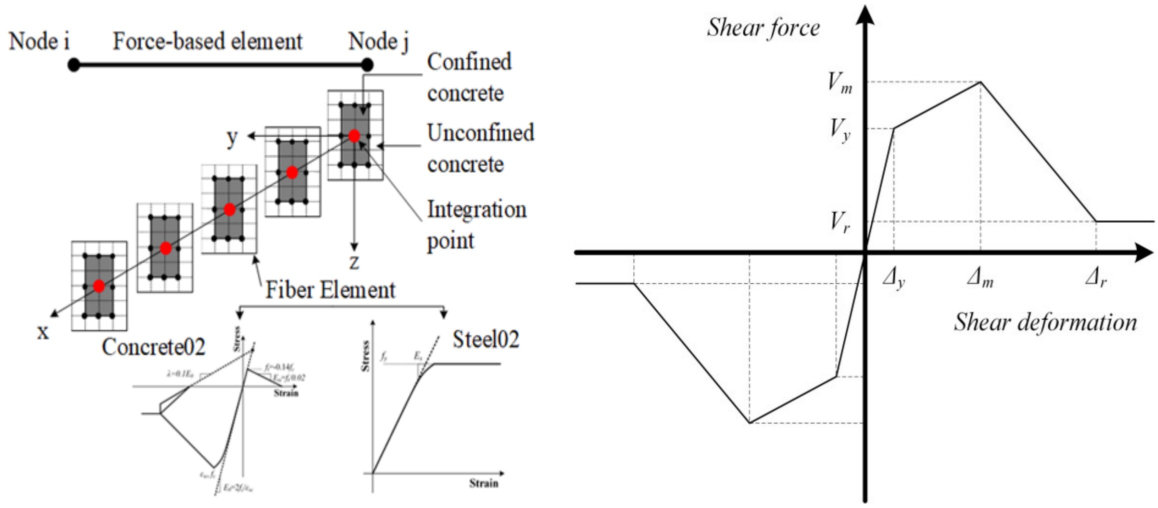

(a) Fiber element (b) Backbone curve of nonlinear shear spring

Fig. 3 – Detail of column flexure-shear model

The maximum shear strength, V_m, of the column was estimated to be 1.137 times that of V_y, based on the literature of Ahmed and Tan [21]. Shear deformation, Δ_m, was 8 times Δ_y at maximum shear strength, residual shear strength Vr was approximately 0.227 times Vy, and shear deformation, Δr, was 16 times of Δy when residual shear strength was reached. Verification of the flexural-shear model of column elements is summarized in section 3.4.

3.3. Equivalent diagonal struct model

The masonry infills installed between the columns were modeled with equivalent diagonal compression struct as shown in Fig. 4. The parameters that determine numerical modeling for equivalent diagonal struct are the effective width (W_{ef}) of the equivalent compression brace, the effective stiffness (K_e), and the maximum strength (F_{max}). The modeling parameters for the equivalent diagonal struct were calculated by using equation (2) to equation (4) on the basis of 1.0B stacking. The crack load (F_{cr}) is assumed to be 0.55Fmax, the tensile strength (F_t) and the residual strength (F_r) are $0.2F_{max}$. The displacement at the maximum strength (δ_{cap}) is assumed to be $2\delta_{cr}$ (crack displacement), and the displacement at the residual strength (δ_r) is assumed to be δ_{cap}.

$$W_{ef} = 0.175(\lambda_h H)^{-0.4}\sqrt{H^2 + L^2} \tag{2}$$

$$K_e = \frac{E_w W_{ef} t_w}{\sqrt{H^2 + L^2}} \cos^2\theta \tag{3}$$

$$F_{max} = 0.818 \frac{L_{in} t_w f_{tp}}{C_I}\left(1 + \sqrt{C_I^2 + 1}\right) \tag{4}$$

where, $\lambda_h = \sqrt[4]{\frac{E_w t_w \sin 2\theta}{4E_c I_c H_{in}}}$, $C_I = 1.925\frac{L_{in}}{H_{in}}$, E_w is elastic modulus of masonry infills (MPa), E_c is elastic modulus of concrete (MPa), t_w is thickness of masonry infills (mm), I_c is second moment of inertia of

© The 17th World Conference on Earthquake Engineering

column element (mm^4), H is height of story (mm), L is column span (mm), H_{in} is effective height of masonry infills (mm), L_{in} is effective length of masonry infills (mm), f_{tp} is crack strength of masonry infills (mm), and θ is slop of diagonal struct.

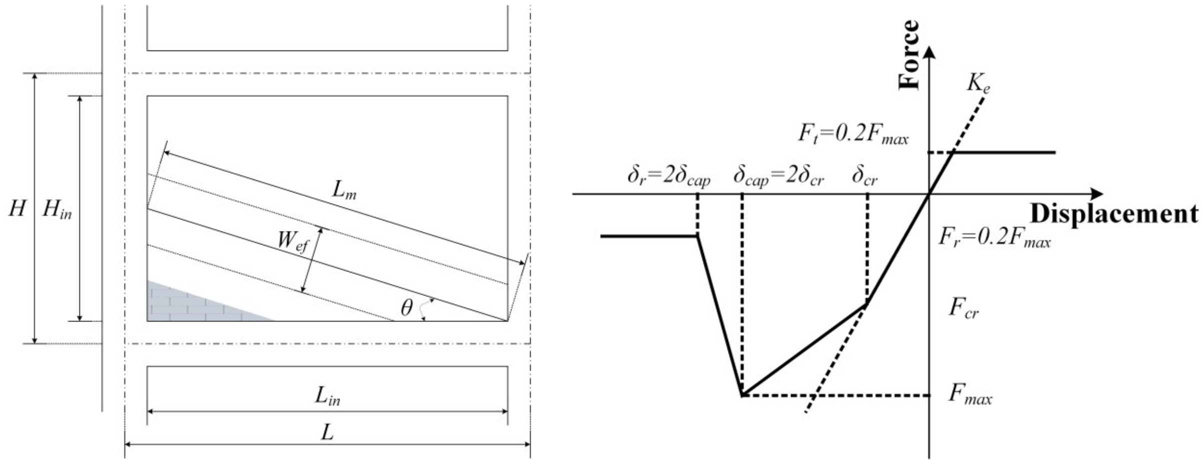

(a) Dimension of masonry infills (b) Backbone curve of nonlinear axial spring

Fig. 4 – Detail of equivalent diagonal struct model

3.4. Numerical model validation

The existing experimental data were investigated to validate the nonlinear column modeling method by comparing the experimental response and the simulation results. The structural properties used for model validation are given in the paper [22].

Fig. 5 represents the comparison of cyclic response of column elements between simulation and experiment. The numerical model used for the column elements well simulates the overall behavior of the experimental specimens. The maximum variations of the initial stiffness and the maximum strength are -3.2% and 5.4% for BG-1 specimen, respectively. A minus sign means that the simulation results are lower than the experimental results. For BG-2 specimen, the maximum variations of the initial stiffness and the maximum strength are -2.6% and -3.2%, respectively. So, it can be concluded that the column model accurately simulates the experimental results in terms of the initial stiffness and maximum strength.

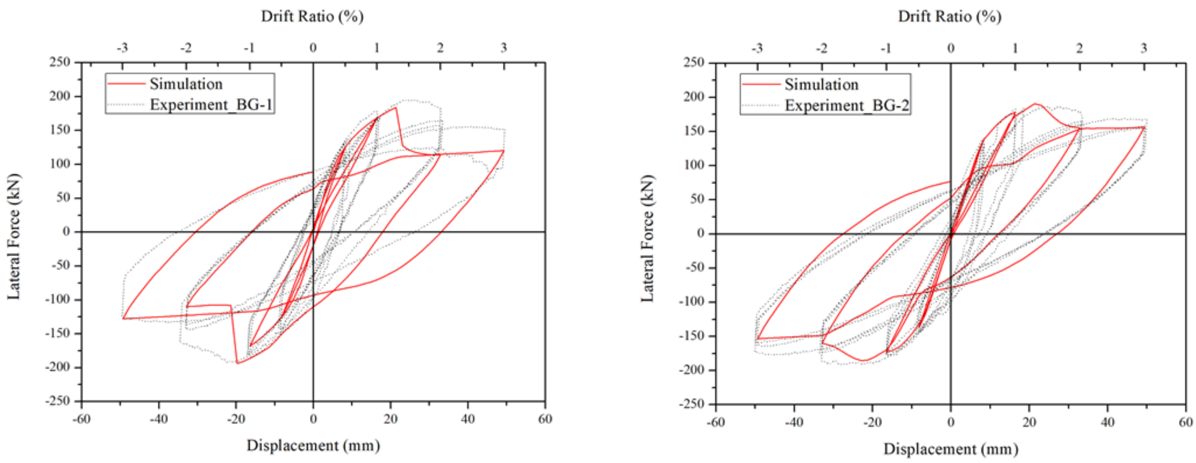

(a) BG-1 (b) BG-2

Fig. 5 – Cyclic response comparison between simulation and experiment [22]

© The 17th World Conference on Earthquake Engineering

4. Evaluation of Seismic Vulnerability Function

4.1. Evaluation of the seismic fragility based on probabilistic demand model analysis

The seismic fragility functions for the structural and nonstructural components are defined using the seismic demand and seismic capacity. When using the probabilistic seismic demand models based on bilinear cloud analysis, the seismic fragility of structural and nonstructural components is evaluated using equation (5).

$$p_f = \Phi\left[\frac{\ln\left(EDP_{IM} / C\right)}{\sqrt{\beta^2_{EDP_{IM}} + \beta^2_C}}\right] \tag{5}$$

where, p_f is the damage probability representing the seismic fragility, $\Phi[\cdots]$ is cumulative distribution of log-normal distribution, EDP_{IM} is the engineering demand parameters such as interstory drift ratio (IDR) or peak floor acceleration (PFA), C is capacity of building components, $\beta^2_{EDP_{IM}}$ is the dispersion of seismic response, and β_C is the dispersion of capacity of building components.

As shown in equation (5), the probabilistic seismic demand models are needed to develop the seismic fragility functions. Generally, the maximum responses of building structure (i.e. maximum interstory drift ratio or maximum peak floor acceleration) had been used as the EDPs for establishing the probabilistic seismic demand model regardless of the number of stories. However, if the damage probabilities of a building structure are measured as a function of seismic fragility using the maximum value, there is a possibility of overestimating the seismic losses resulting from the seismic damage occurring in each story [23]. Therefore, in this study, the seismic demands were assessed using the probabilistic seismic demand model using the bilinear least square fitting method (i.e. the bilinear cloud analysis [24]). Also, a total of 44 far-field ground motion data (22 pairs) were used to perform the nonlinear time history analysis for the prototype model. The probabilistic seismic demand models for IDR and PFA are established using the results of the time history analysis.

Fig. 6 showed the probabilistic seismic demand models of IDR and PFA for 1st floor. While the linear cloud method is presented by a power function, the bilinear cloud method used in this study is presented by two power function. Typically, if the building experiences a certain EDP (i.e. IDR or PFA) enough to failure the structural or the nonstructural components, the EDP was rapidly increased with respected to the seismic intensity. As shown in Fig. 6, it can be seen that there is a rapid increase in IDR and PFA when S_a is 0.4g or more. In other words, the bilinear method is more appropriate to estimate the seismic response than the linear method in case of major damage to the building structure.

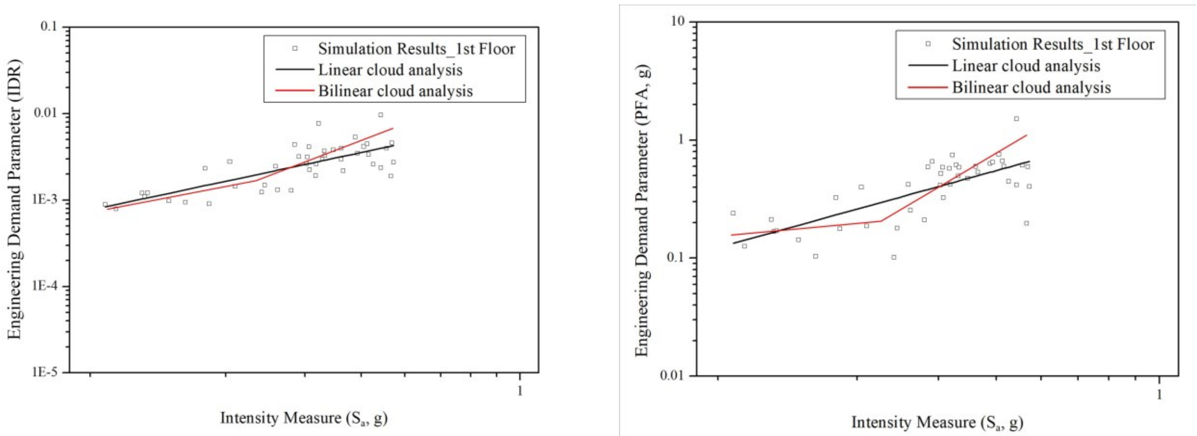

(a) IDR (b) PFA

Fig. 6 – Probabilistic seismic demand models of IDR and PFA for 1st floor

© The 17th World Conference on Earthquake Engineering

The correlation analysis with simulation data were performed to statistically evaluate the reliability of the probabilistic seismic demand models obtained the two methods. The simulation data were used as the reference data. The results of the correlation analysis are summarized in Table 2. The coefficient of determination (R^2) was introduced as a measurement to quantitatively evaluate the correlation between seismic demand models and simulation data. The R^2 derived from the linear cloud method for the IDR on the first story is 0.5944 and the R^2 derived from the bilinear cloud method is 0.7819, which shows that the bilinear method well estimates the seismic response with higher reliability than the linear cloud method. Therefore, the probabilistic seismic demand models based on bilinear cloud analysis are used for seismic fragility analysis.

Table 2 – Results of correlation analysis for probabilistic seismic demand model

Engineering Demand Parameter	**Story Level**	**Coefficient of Determination (R^2)**	
		Linear Cloud	**Bilinear Cloud**
Interstory drift ratio	1	0.5944	0.7819
	2	0.6512	0.7365
	3	0.6848	0.8250
Peak floor acceleration	1	0.6352	0.8235
	2	0.6634	0.7870
	3	0.6766	0.7929

The limit states for the structural and architectural nonstructural components are determined to define the seismic fragility functions. The median and the dispersion of structural and nonstructural components must be defined to estimate the seismic fragility functions (see equation (5)). Usually, the median value of the structural components (i.e. damage level according to the limit states) is defined as a maximum interstory drift ratio. The damage states of school building structures used in this study are summarized in Table 3 through the existing literature review [16, 25].

Table 3 – Capacity parameters of structural and nonstructural component in school building

Building Component	**Parameter**	**Unit**	**DS1**		**DS2**		**DS3**	
			C	β_C	***C***	β_C	***C***	β_C
Structural component	IDR	-	0.0035	0.40	0.0070	0.40	0.0120	0.40
Masonry infills	IDR	-	0.0021	0.60	0.0071	0.45	0.0120	0.45
Partitions	IDR	-	0.0064	0.30	-	-	-	-
Tiles	IDR	-	0.0021	0.60	0.0071	0.45	-	-
Ceilings	PFA	g	0.7	0.25	1.2	0.25	1.43	0.25
Floor finishing	PFA	g	0.5	0.40	0.7	0.40	-	-

The seismic fragility functions for the structural and nonstructural components were derived from the seismic demand and the limit states to probabilistically evaluate the physical damage of the school building structures (see Fig. 7). The exceedance probabilities of structural components reaching DS1 are similar in the first and second stories, and those of structural components reaching DS2 and DS3 are highest in the first story. According to the earthquake reconnaissance of the school building structures [7], the major damages were observed in the column elements of the first story, and no significant damages were observed as the number of stories increased. Therefore, the seismic fragility functions presented in this study reflect well the damage patterns observed in the school building structures. In section 4.2, the seismic vulnerability function

© The 17th World Conference on Earthquake Engineering - 8b-0014 -

was evaluated to analysis the seismic loss of school building using the structural and nonstructural seismic fragility functions representing the physical damages.

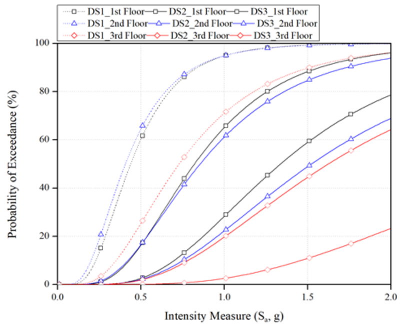

(a) Structural component

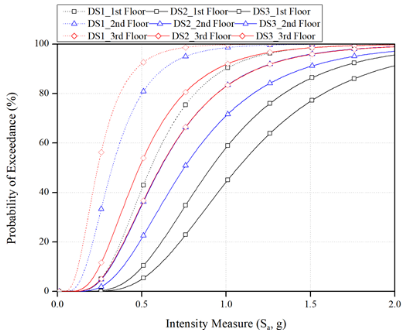

(b) Masonry infills

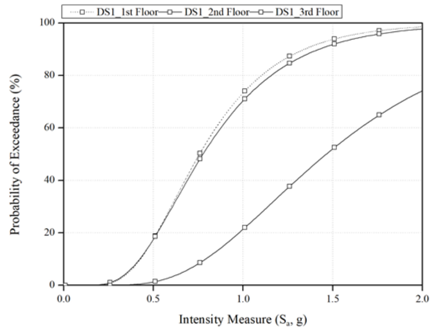

(c) Partitions

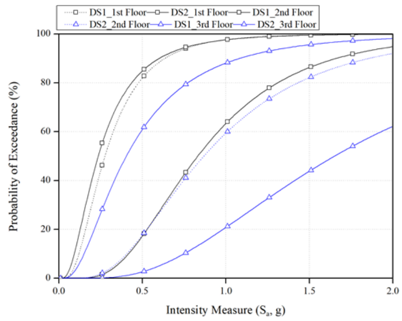

(d) Tiles

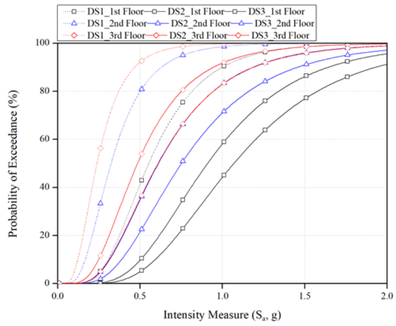

(e) Ceiling

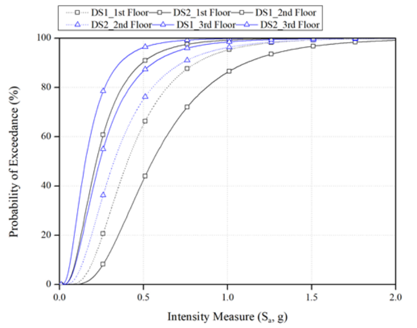

(f) Floor finishing

Fig. 7 – Structural and nonstructural seismic fragility functions for each story

4.2. Seismic loss analysis of the school building

The seismic vulnerability function for the school building must be defined in order to estimate the direct loss induced by earthquake. The repair cost regarding each damage state for structural and nonstructural components were investigated to define the seismic vulnerability function from literature [25] and summarized in Table 4.

Table 4 – Loss estimation parameters for structural and nonstructural components

Building Component	Unit of Measurement	Quantity	Mean Repair Cost (₩/unit of measurement)		
			DS1	DS2	DS3
Structural component	m^2	55	2,300,172	3,645,325	4,360,324
Masonry infills	m	83.1	233,200	604,998	2,173,876
Partitions	m	204	311,175	-	-
Tiles	m	55.9	777,331	3,296,747	-
Ceilings	m^2	43.9	280,500	2,188,496	4,726,505
Floor finishing	m^2	537	72,149	121,465	-

Fig. 8(a) showed the seismic vulnerability function using simulation data. The vertical axis represents the damage ratio defined by the ratio of repair cost and replacement cost. Each point in Fig. 8(a) are the

© The 17th World Conference on Earthquake Engineering

result calculated from the mean repair costs summarized in Table 5 and the seismic fragility functions summarized in Section 4.1. The median and the standard deviation (i.e. vulnerability function parameter) are 0.8912, and 0.4257, respectively. The damage ratio of individual building can be evaluated from the defined seismic vulnerability function a particular scenario earthquake. For example, in the case of Gyeongju Earthquake (S_a is 0.3g), the damage ratio is 1.32% (see Fig. 8(b)). So, it is possible to estimate the damage ratio per each component for each story.

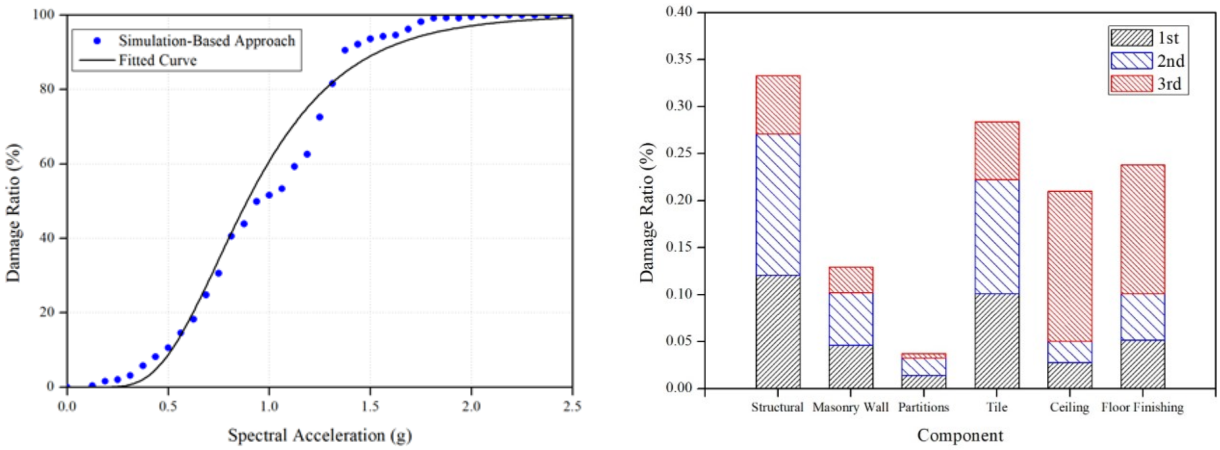

(a) Seismic vulnerability function (b) Component damage ratio (S_a=0.3g)

Fig. 8 – Seismic vulnerability function of the school building

4.3. Evaluation of loss-based seismic performance of the school building

In order to assess the seismic performance of building structures based on seismic losses, it is necessary to define a loss-based seismic performance criteria. Analyzing the trend of damage ratio for seismic intensity, the damage ratio of school building increases sharply from 8.79% at 0.5g to 60.79% at 1.0g (see Fig. 8(a)). The main reason for this increase of damage ratio is the high interstory drift ratio caused by the shear failure of the column on the 1st and 2nd stories. Therefore, it is possible to define the loss-based seismic performance criteria through correlation analysis between the interstory drift ratio (physical damage) and the damage ratio (economic loss).

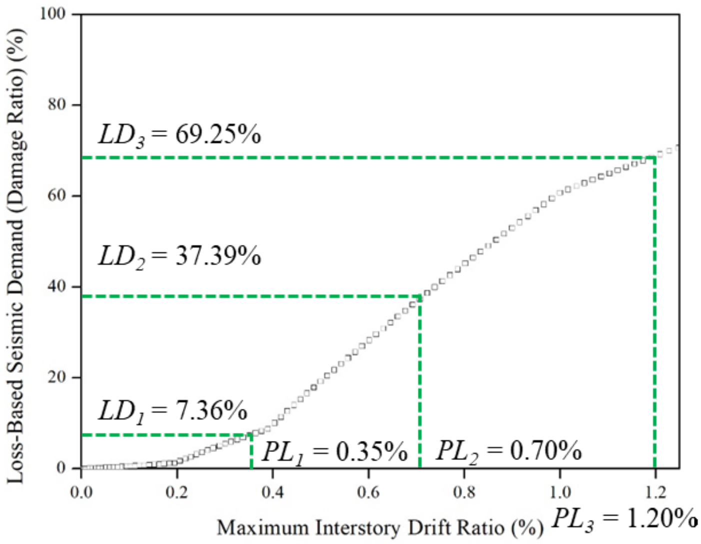

Fig. 9 – Loss-based performance limits corresponding to current code-defined performance levels

© The 17th World Conference on Earthquake Engineering

Current seismic performance evaluation method suggests the performance limit based on the interstory drift ratio of the structural components. In this study, the loss-based performance criteria are presented as shown in Figure 9 by directly connecting the displacement-based performance limit suggested in the current code with the seismic loss. The performance limits based on interstory drift ratio for the school buildings (PL_i) are divied in to PL_1=0.35%, PL_2=0.70%, and PL_3=1.20%, and the corresponding loss-based performance limit (LD_i) can be defined as LD_1=7.36%, LD_2=37.39%, and LD_3=69.25%. The damage ratio and corresponding current seismic performance of the school building are simmarized in Table 5. The estimated seismic loss for S_a=0.494g, which corresponds to the design load level, is 39.01%, and the seismic performance of the school building that caused these seismic loss is interpreted as the collapse prevention from the current seismic performance level.

Table 5 – Loss-based performance evaluation of the school building

Divisions	**20%**	**40%**	**Design (66.7%)**	**80%**	**MCE**
Seismic intensity (S_a)	0.150	0.300	0.494	0.600	0.750
Damage ratio (%)	7.60%	19.50%	39.01%	48.56%	67.70%
Corresponding current performance	LS	LS	CP	CP	CP

5. Conclusions

In this study, a simulation-based framework for evaluating the seismic vulnerability function is presented and applied to the school building. The flexure-shear behavior of column elements is presented to simulate the premature shear failure and validated with the experimental data. The seismic fragility functions for structural and nonstructural elements are evaluated to assess seismic vulnerability function. Using repair cost ratio that quantify structural and nonstructural damage as a percentage of total replacement cost, the seismic vulnerability function regarding the seismic intensity is defined. Also, the loss-based performance criteria are proposed through the correlation analysis between the current displacement-based performance limit and the seismic loss. The seismic losses of the school building are 39.01% for design load level and 67.70% for maximum considered earthquake (MCE) load level. In conclusions, it is found that the proposed methodology can provide decision-making data for evaluating seismic performance based on seismic loss and has the potential to extend to loss assessment of other categories of buildings.

6. Acknowledgements

This research was supported by a grant (NRF-2018R1A2B6006958) from the National Research Foundation of Korea (NRF) funded by the Korean Ministry of Science and ICT (MSIT).

7. References

[1] Vision 2000 Committee (1995): *Performance Based Seismic Engineering of Buildings*, Structural Engineers Association of California (SEAOC).

[2] ATC 40 (1996): *Seismic Evaluation and Retrofit of Existing Concrete Buildings*, Applied Technical Council.

[3] Shin J, Kim JH, Lee, KH (2014): Seismic Assessment of Damaged Piloti-Type RC Building Subjected to Successive Earthquakes. *Earthquake engineering & Structural dynamics*, **43**(11) 1603-1619.

[4] Rihal S (1992): Correlation Between Recorded Building data and Nonstructural Damage During the Loma Prieta Earthquake of October 19, 1989–Selected Case Studies. *In Proceedings of the 10th World Conference on Earthquake Engineering*. 1, 73-78.

© The 17th World Conference on Earthquake Engineering

[5] Ayres JM, Sun TY (1973): Nonstructural Damage, The San Fernando, California Earthquake of February 9, 1971, Washington, D.C.

[6] Bradley BA, Dhakal RP, Cubrinovski M, MacRae GA, Lee DS (2009): Seismic Loss Estimation for Efficient Decision Making. *Bulletin of the New Zealand Society for Earthquake Engineering*, **42**(2) 96–110.

[7] Kim HJ, Baek ER, Kim YS, Lee SH (2019): An Analysis Study on the School Buildings Damaged by the Pohang Earthquake (in Korean). *Journal of the Regional Association of Architectural Institute of Korea*, **21**(1) 15-23.

[8] Cho HC (2018): The Distribution of Safety within a State: Seismic Evaluation of School Buildings. *Korean Journal of Policy Studies*, **33**(1) 1-32.

[9] Miranda E, Aslani H (2003): *Probabilistic Response Assessment for Building-Specific Loss Estimation*. Pacific Earthquake Engineering Research Center.

[10] Hutchinson TC, Restrepo JI, Conte JC, Pantoli E, Chen MC, Wang X, Astroza R, Ebrahimian H (2014): Shake Table Testing of a Five Story Building Outfitted with NCSs (BNCS project). *Network for Earthquake Engineering Simulation (distributor), Dataset*. DOI: 10.4231/D38W38349

[11] Astroza R, Pantoli E, Selva F, Restrepo JI, Hutchinson TC, Conte JP (2015): Experimental Evaluation of the Seismic Response of a Rooftop-Mounted Cooling Tower. *Earthquake Spectra*, **31**(3) 1567-1589.

[12] Soroushian S, Maragakis EM, Ryan KL, Sato E, Sasaki T, Okazaki T, Mosqueda G (2015): Seismic Simulation of an Integrated Ceiling-Partition Wall-Piping System at E-Defense. II: Evaluation of Nonstructural Damage and Fragilities. *Journal of Structural Engineering*, **142**(2) 04015131.

[13] Guzman Pujols JC, Ryan, KL (2015): Data from the Network for Earthquake Engineering Simulation/E-Defense Collaborative Test Program on Innovative Isolation Systems and Nonstructural Components. *Earthquake Spectra*, **31**(2), 1195-1209.

[14] MOIS (2017): *2016-2017 Property Loss by Disaster (in Korean)*. The Ministry of the Interior and Safety.

[15] Lee JW (2008): A Study on the Standard Drawings of Seoul Elementary School Architecture in 1960~1970s (in Korean). *Journal of the Korea Academia-Industrial Cooperation Society*, **9**(6) 1718-1725.

[16] MLTM (2011): *Seismic Performance Evaluation for Existing Buildings (in Korean)*, Ministry of Land, Transport and Maritime Affairs, Korea

[17] McKenna F, Scott MH, Fenves GL (2010): Nonlinear Finite-Element Analysis Software Architecture Using Object Composition, *Journal of Computing in Civil Engineering*, **24** 95-107

[18] Vahidi EK, Malekabadi MM (2009): Conceptual Investigation of Shortcolumns and Masonry Infill Frames Effect in the Earthquakes. *International Journal of Civil and Environmental Engineering*, **3**(11) 472-477.

[19] Fiore A, Netti A, Monaco P (2012): The influence of masonry infill on the seismic behaviour of RC frame buildings. *Engineering structures*, **44** 133-145.

[20] FEMA 356 (2000): *Prestandard and Commentary for the Seismic Rehabilitation of Buildings*, Federal Emergency Management Agency.

[21] Ahmed A, Tan KH (2014): Development of Displacement Based Shear Hinge for Shear Controlled RC Components, *Structural Engineering Convention (SEC): International Workshop on Emerging Trends in Earthquake Engineering and Structural Dynamics*, New Delhi, India.

[22] Saatcioglu M, Grira M (1999): Confinement of Reinforced Concrete Columns with Welded Reinforced Grids. *Structural Journal*, **96**(1) 29-39.

[23] Ramamoorthy SK, Gardoni P, Bracci JM (2006): Probabilistic Demand Models and Fragility Curves for Reinforced Concrete Frames. *Journal of Structural Engineering*, **132**(10) 1563-1572.

[24] Bai JW, Gardoni P, Hueste MBD (2011): Story-Specific Demand Models and Seismic Fragility Estimates for Multi-Story Buildings. *Structural Safety*, **33**(1) 96-107.

[25] FEMA P58-1. (2012): *Seismic performance assessment of buildings: 1–Methodology*. Prepared by the Applied Technology Council for the Federal Emergency Management Agency.

© The 17th World Conference on Earthquake Engineering